Molecular Therapy
Nucleic Acids
Original Article

Aberrant elevation of GDF8 impairs granulosa cell glucose metabolism via upregulating SERPINE1 expression in patients with PCOS

Long Bai,[1,2,3] Wei Wang,[1,2,3] Yu Xiang,[1,2] Shuyi Wang,[1,2] Shan Wan,[1,2] and Yimin Zhu[1,2]

[1]Department of Reproductive Endocrinology, Women's Hospital, School of Medicine, Zhejiang University, Hangzhou, Zhejiang 310002, China; [2]Key Laboratory of Reproductive Genetics (Ministry of Education) and Women's Reproductive Health Laboratory of Zhejiang Province, Women's Hospital, Zhejiang University School of Medicine, Hangzhou, Zhejiang 310002, China

Clinical investigations have demonstrated that polycystic ovary syndrome (PCOS) is often accompanied by insulin resistance (IR) in more than 70% of women with PCOS. However, the etiology of PCOS with IR remains to be characterized. Growth differentiation factor 8 (GDF8) is an intraovarian factor that plays a vital role in the regulation of follicle development and ovulation. Previous studies have reported that GDF8 is a pathogenic factor in glucose metabolism disorder in IR patients. To date, the role of GDF8 on glucose metabolism of granulosa cell in PCOS patients remains to be determined. In the current study, we demonstrated that the expression and accumulation of GDF8 in human granulosa-lutein (hGL) cells and follicular fluid from PCOS patients were higher compared with those of non-PCOS women. GDF8 treatment caused glucose metabolism defects in hGL cells. Transcriptome sequencing results showed that SERPINE1 mediated GDF8-induced impairment of hGL glucose metabolism defects. Using pharmacological and small interfering RNA (siRNA)-mediated knockdown approaches, we demonstrated that GDF8 upregulated the expression of SERPINE1 via the ALK5-mediated SMAD2/3-SMAD4 signaling pathway. Interestingly, the extracellular signal-regulated kinase 1/2 (ERK1/2) signaling pathway was also activated with GDF8 treatment but did not participate in the effect of GDF8 on SERPINE1 expression. Our results also showed that TP53 was required for the GDF8-stimulated increase in SERPINE1 expression. Importantly, our study demonstrated that SB-431542 treatment significantly improved DHEA-induced PCOS-like ovaries. These findings support a potential role for GDF8 in metabolic disorders in PCOS.

INTRODUCTION

Polycystic ovary syndrome (PCOS) is one of the most common and heterogeneous endocrinopathies and severely influences women's reproductive performance.[1] PCOS is diagnosed by the characteristics of clinical or biochemical hyperandrogenism, polycystic ovarian morphology, and ovulatory dysfunction.[2] Moreover, PCOS is commonly associated with obesity and accompanies body-wide insulin resistance (IR).[3] Clinical investigations show that the prevalence of IR is approximately 70% among PCOS patients, indicating the close relevance of IR to PCOS development.[4] IR is an endocrine metabolic disorder that is characterized as a requirement for an accumulation of insulin to achieve a given metabolic action as a result of the impaired function of insulin in regulating glucose uptake and metabolic production.[5] In general, IR is conventionally defined as the decreased ability of insulin in glucose utilization by peripheral tissues, particularly adipose tissue and muscle.[5] In recent years, increasing evidence has suggested that glucose metabolism disorders in granulosa cells trigger the occurrence and development of PCOS.[2,6,7] However, the underlying mechanism of glucose uptake defects in PCOS patient granulosa cells remains unknown.[7,8] The follicle is the core functional unit of the ovary and is composed of a single oocyte with surrounding somatic cells, including granulosa cells, cumulus cells, and theca cells. During the female reproductive cycle, oocytes maintain a state of meiotic arrest and bidirectionally communicate with granulosa cells before gonadotropin stimulation.[9] The normal glucose metabolism of granulosa cells is indispensable for follicular development by providing essential energy substrates and intermediates to support oocyte development and maturation.[10] Maintenance of the metabolic function of granulosa cells relies on the dynamic balance of the follicular microenvironment under the control of multiple growth factors derived from granulosa cells. Aberrant expression of cytokines in granulosa cells, which are the main component of follicles, disrupts the balance of the follicular microenvironment; this further leads to abnormalities in follicle development by disrupting the function of granulosa cells.

Received 7 June 2020; accepted 5 November 2020;
https://doi.org/10.1016/j.omtn.2020.11.005.

[3]These authors contributed equally

Correspondence: Yimin Zhu, MD, PhD, Department of Reproductive Endocrinology, Women's Hospital, School of Medicine, Zhejiang University, Hangzhou 310006, China.
E-mail: zhuyim@zju.edu.cn
Correspondence: Long Bai, PhD, Department of Reproductive Endocrinology, Women's Hospital, School of Medicine, Zhejiang University, Hangzhou 310006, China.
E-mail: bailong0375@zju.edu.cn

Growth differentiation factor 8 (GDF8), also named myostatin, is a member of the transforming growth factor-β (TGF-β) superfamily and was originally identified as a mediator that participates in the regulation of skeletal muscle development.[11] Recent studies have demonstrated the role of GDF8 in the mammalian reproductive system, including the regulation of follicle development, steroidogenesis, and granulosa cell proliferation and differentiation.[12] The serum GDF8 levels exhibit dynamic changes during the controlled ovarian hyperstimulation in *in vitro* fertilization (IVF) patients. The concentration of GDF8 in serum is decreased dramatically from hCG day to oocyte pick-up day, implying that the low GDF8 level is necessary for successful ovulation. Furthermore, many studies in adipocytes and myocytes highlight the function of GDF8 in the regulation of cellular metabolism, such as insulin-mediated cellular glucose metabolism. In particular, GDF8 has a positive role in the pathophysiology of several metabolic disorders, including obesity, IR, and diabetes.[13–16] Additionally, clinical studies have indicated that aberrantly high expression of GDF8 in the placenta of preeclampsia women indicates the involvement of GDF8 in female reproductive disorders.[17] In PCOS women, serum GDF8 levels are higher in the PCOS group than in the control group. Intriguingly, a high level of GDF8 is found only in obese PCOS women, whereas there is no difference between nonobese women regardless of PCOS status.[18] Our most recent study shows that GDF8 and its known receptors, ACVR2A, ACVR2B, and TGFBR, are localized in human antral follicles, and that expression of this protein increases with follicle diameter. Moreover, the expression level of GDF8 in granulosa cells and theca cells is increased in PCOS ovaries, suggesting that the aberrant expression of GDF8 is involved in the pathogenesis of PCOS.[19] Given that GDF8 is a pathogenic factor in glucose metabolism disorders, we hypothesize that GDF8 is a potential mediator involved in insulin-dependent metabolic defects in granulosa cells of PCOS patients. In the current study, we sought to explore the role of GDF8 in PCOS patient metabolic disorders and the underlying molecular mechanism.

RESULTS

GDF8 levels are higher in women with PCOS than in the control group

Increasing evidence suggests that aberrant changes in growth factors in the intrafollicular microenvironment lead to abnormal follicle development in PCOS.[20] Previous studies have shown that peripheral blood GDF8 levels are higher in individuals with PCOS than in those without PCOS.[18] However, little is known about the changes in GDF8 levels in the follicular microenvironment. To determine the changes in GDF8 levels in the follicular microenvironment, we collected human follicular fluid with oocyte retrieval from PCOS and non-PCOS IVF patients. The GDF8 concentration was measured using the GDF8 enzyme-linked immunosorbent assay (ELISA) kit. Our results showed that the GDF8 concentration was significantly higher in the PCOS group than in the non-PCOS group (Figure 1A). We subsequently analyzed all follicular fluid GDF8 concentration data stratified by the HOMA-IR index. We found that GDF8 was significantly higher in IR women with PCOS than in non-IR women with PCOS, whereas there was no difference between IR and non-IR women in control groups (Figure 1B). Moreover, the differences in GDF8 concentrations in follicular fluid between control obese and PCOS obese patients were also analyzed. We found that GDF8 levels were also higher in PCOS obese patients than in the control obese group (Figure 1C). Next, we analyzed the correlations of all follicular fluid GDF8 concentration data according to androgen concentration and body mass index (BMI) in PCOS patients. Our results showed that GDF8 concentration was positively correlated with BMI (Figure 1D). Interestingly, although GDF8 concentration was negatively correlated with androgen concentration in PCOS patients, the p value did not reach significance level (Figure 1E). Additionally, primary hGL cells from PCOS and non-PCOS patients were also collected, and GDF8 expression levels were detected using quantitative PCR (qPCR). The qPCR results showed that the expression levels of GDF8 were higher in the PCOS group than in the non-PCOS group (Figure 1F), which was consistent with our previous human ovary immunohistochemistry results showing that PCOS patient ovaries display aberrantly increased GDF8 expression levels.[19]

GDF8 levels are negatively correlated with IVF outcome

GDF8 is a mediator that participates in folliculogenesis and has been widely reported.[12] To date, few studies have evaluated the possibility that GDF8 is an IVF outcome predictor. In the present study, we collected the clinical information of IVF patients and analyzed the relationship between GDF8 concentration and IVF outcomes. The results showed that GDF8 levels were negatively correlated with the number of oocytes obtained from IVF patients (Figure 1G), fertilization rate (Figure 1H), and rate of high-quality embryos (Figure 1I), indicating that GDF8 level in follicular fluid may be a potential predictor to assess IVF outcomes.

GDF8 impairs glucose metabolism in hGL cells

Animal studies have proved that GDF8 is a negative mediator involved in body-wide IR and regulates skeletal muscle cell glucose metabolism.[21] To determine the effect of GDF8 on hGL cell glucose metabolism, we treated primary hGL cells with GDF8 and measured the amount of glucose uptake. The selection of GDF8 concentration in all of the following experiments was according to our clinical results and previous studies from other research groups. In our clinical studies, the concentration of GDF8 in human follicular fluid ranged from 1 to 8 ng/mL. Meanwhile, it has been reported that 30 ng/mL GDF8 could significantly affect primary hGL cell function.[22] Thus, a 30 ng/mL concentration of GDF8 was used in our study. The glucose uptake analysis results showed that GDF8 inhibited insulin-induced glucose uptake in hGL cells (Figure 2A). Lactate accumulation levels were also detected using a lactate analysis kit, and the results showed that GDF8 also abolished insulin-induced lactate production (Figure 2B). Furthermore, changes in the expression level of insulin signaling pathway-related proteins in response to GDF8 treatment were also examined. Quantitative real-time RT-PCR results showed that GDF8 did not affect the expression of insulin signaling pathway-related proteins, including IRS-1, IRS-2, INSR, and GLUT4 (Figure 2C).

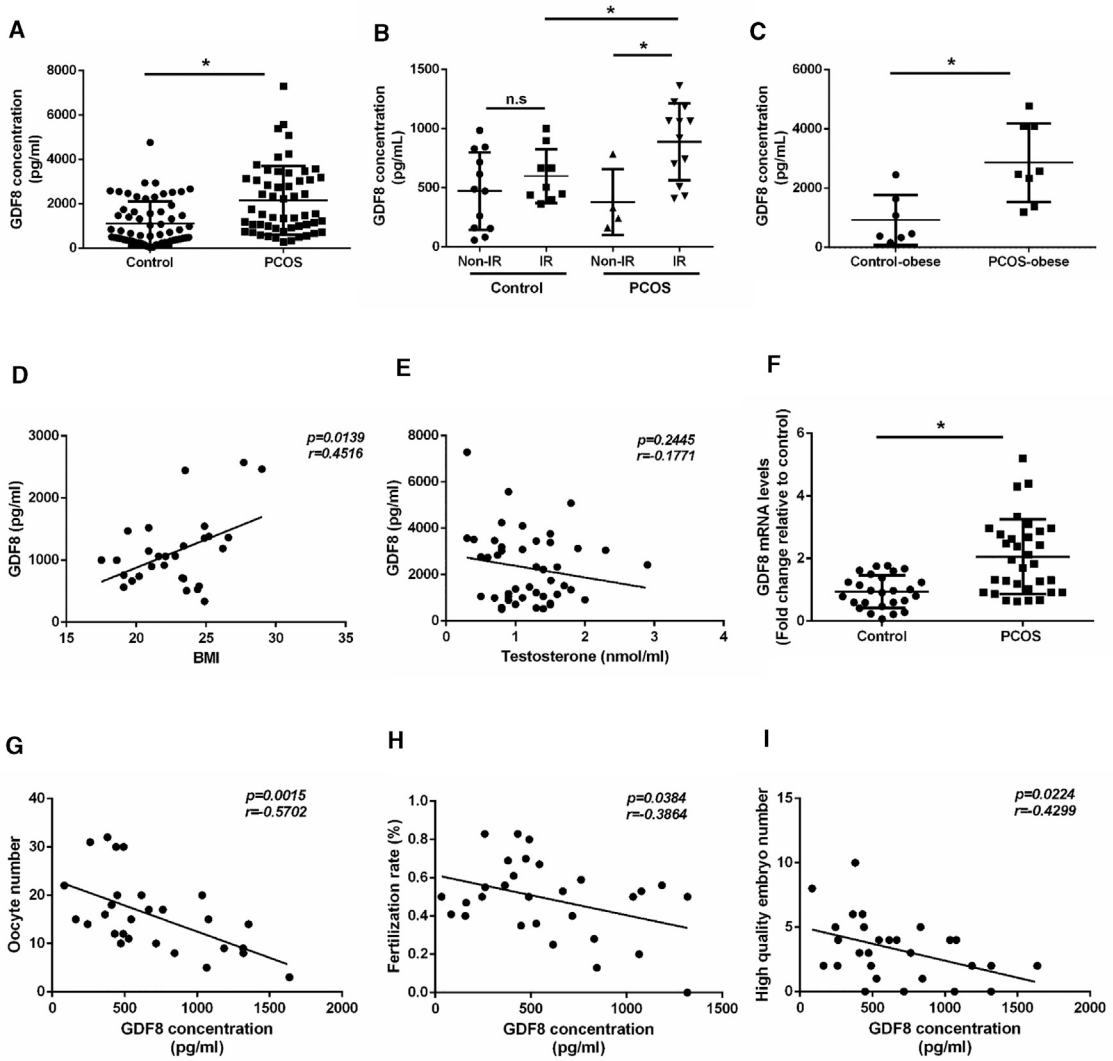

Figure 1. GDF8 levels are higher in women with PCOS than those in the control group

(A) The difference of GDF8 concentrations in follicular fluid between PCOS patients and control groups. (B) GDF8 concentrations in follicular fluid derived from control and PCOS patients with or without IR. (C) Comparison of GDF8 levels in obese patients with or without PCOS. (D and E) The correlation analysis of GDF8 levels with BMI or testosterone in PCOS patients, respectively. (F) The mRNA expression change analysis of GDF8 in granulosa cells derived from control or PCOS patients. (G–I) The correlation analysis of GDF8 levels with IVF outcomes, including obtained oocyte number, fertilization rate, and high-quality embryo number. One-way analysis of variance (ANOVA) followed by Duncan test for multiple comparisons of means. Meanwhile, for experiments involving only two groups, the data were analyzed by the two-sample t test assuming unequal variances. $p < 0.05$ was considered statistically significant.

SERPINE1 is involved in GDF8-induced disruption of glucose metabolism in hGL cells

To identify the potential key factor involved in GDF8-induced disruption of glucose metabolism, we treated primary hGL cells with GDF8 for 12 h and then prepared an RNA sequencing (RNA-seq) library. RNA-seq methods were used to examine changes in the transcriptome level in hGL cells. Transcriptome analysis results showed that 401 were upregulated and 90 genes were downregulated (Figure 2D). The enrichment and Gene Ontology (GO) analyses of the sequencing results showed that the changed genes were enriched for cell metabolic process, such as glycosaminoglycan metabolic process and aminoglycan metabolic process (Figures 2E and 2F). Meanwhile, Disease Ontology (DO) analyses were also performed to explore the change of genes involved in human disease, and the results showed that 12 PCOS-related genes, 12 infertility-related genes, and 4 hyperandrogenism-related genes were changed (Figure 2G). Comprehensive analysis of all genes in these three types of disease identified SERPINE1 as a potential factor that may be involved in the regulatory effect of GDF8 on granulosa cell pathophysiology as a result of the presence of SERPINE1 in three different pathological activities (Figure 2H). Next, seven genes (upregulated or downregulated) with expression changes in response to GDF8 treatment were selected to further confirm the RNA-seq results using

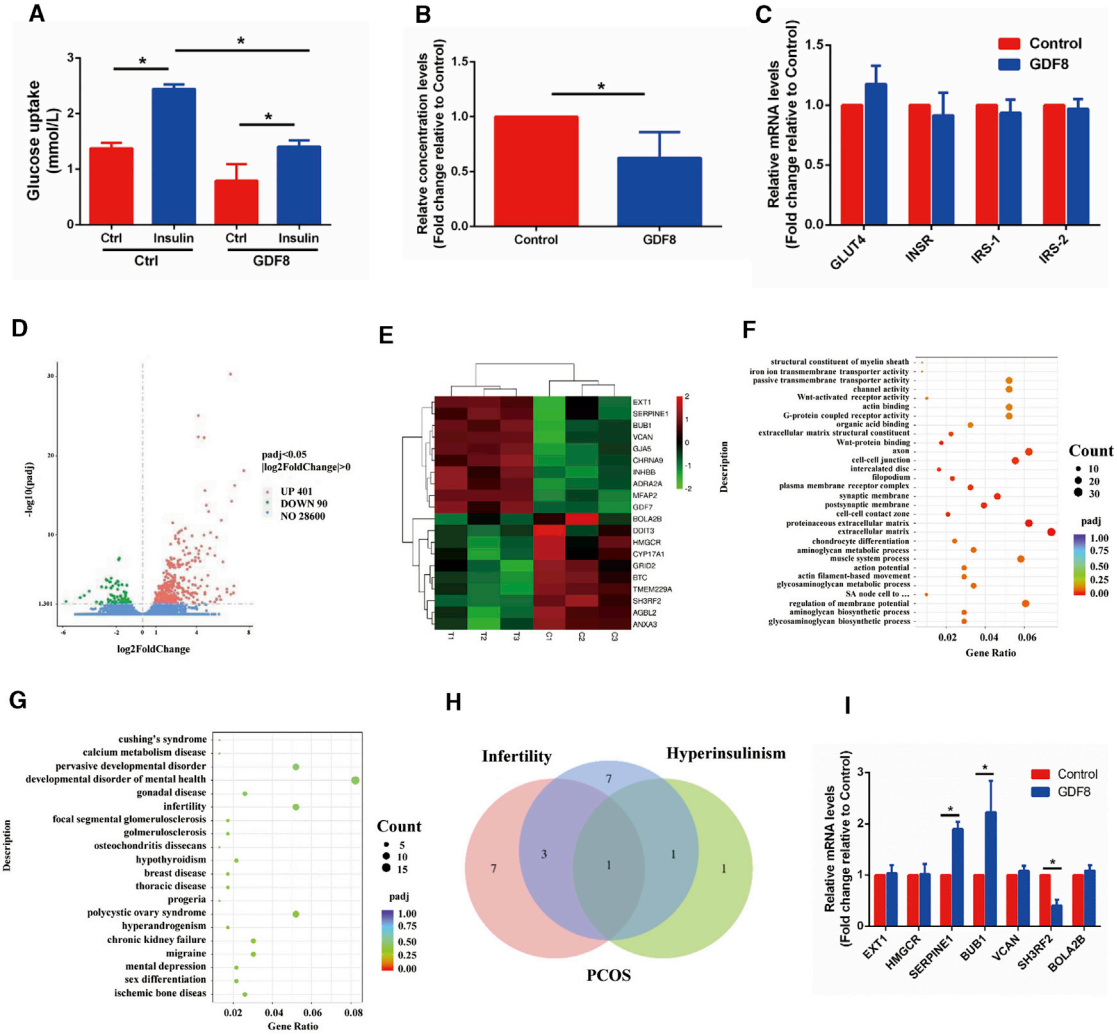

Figure 2. GDF8 impairs insulin-dependent glucose metabolism in hGL cells

(A) The hGL cells were pretreated with vehicle control or GDF8 (30 ng/mL) for 24 h and then treated with insulin (300 nM) for an additional 1 h, and the changes of glucose intake were measured. (B) The hGL cells were treated with vehicle control or GDF8 for 24 h, and the levels of lactate were detected. (C) The hGL cells were pretreated with vehicle control or GDF8 (30 ng/mL) for 12 h, and the gene expression changes related to insulin signaling pathway were examined by quantitative real-time RT-PCR. (D) Volcano plot of RNA-seq data from control and GDF8-treated hGL cells. (E) Cluster analysis of differential expression genes from RNA-seq data in control and GDF8-treated hGL cells. (F) The enriched Gene Ontology terms of biological process categories of differential expression genes from RNA-seq data in control and GDF8-treated hGL cells. (G) The enrichment analysis of human disease-related genes using Disease Ontology methods. (H) Venn diagram depicting the overlap of expression change genes in different groups. (I) The expression changes of genes (upregulated or downregulated) from RNA-seq data in control and GDF8-treated hGL cells. The differential gene expression was identified using DESeq2 software. Significant differentially expressed genes (DEGs) were examined with padj (adjusted p value) < 0.05. Meanwhile, absolute fold change of 2 was set as the threshold for significant differential expression. One-way ANOVA followed by Duncan test for multiple comparisons of means. Meanwhile, for experiments involving only two groups, the data were analyzed by the two-sample t test assuming unequal variances. $p < 0.05$ was considered statistically significant.

quantitative real-time RT-PCR. Our results showed that SERPINE1 and BUB1 mRNA expression levels were increased and SH3RF2 expression levels were decreased with GDF8 treatment in both KGN and hGL cells, whereas expression of EXT1, HMGCR, VCAN, and BOLA2B did not change (Figure 2I). To examine the difference in SERPINE1 concentration in follicular fluid between control and PCOS women, we randomly selected 26 samples in the control group and 28 samples in the PCOS group to detect the concentration of SERPINE1 in follicular fluid. Our results found that SERPINE1 concentration was significantly higher in the PCOS group than in the non-PCOS group (Figure 3A). Meanwhile, the correlation between GDF8 and SERPINE1 concentration was also analyzed, and results showed that even through there was a positive correlation trend with SERPINE1 concentration, the p value did not reach significance level (Figure 3B). Next, the protein expression changes in SERPINE1 at different time points (12 or 24 h) after GDF8 treatment were further analyzed in hGL cells using western

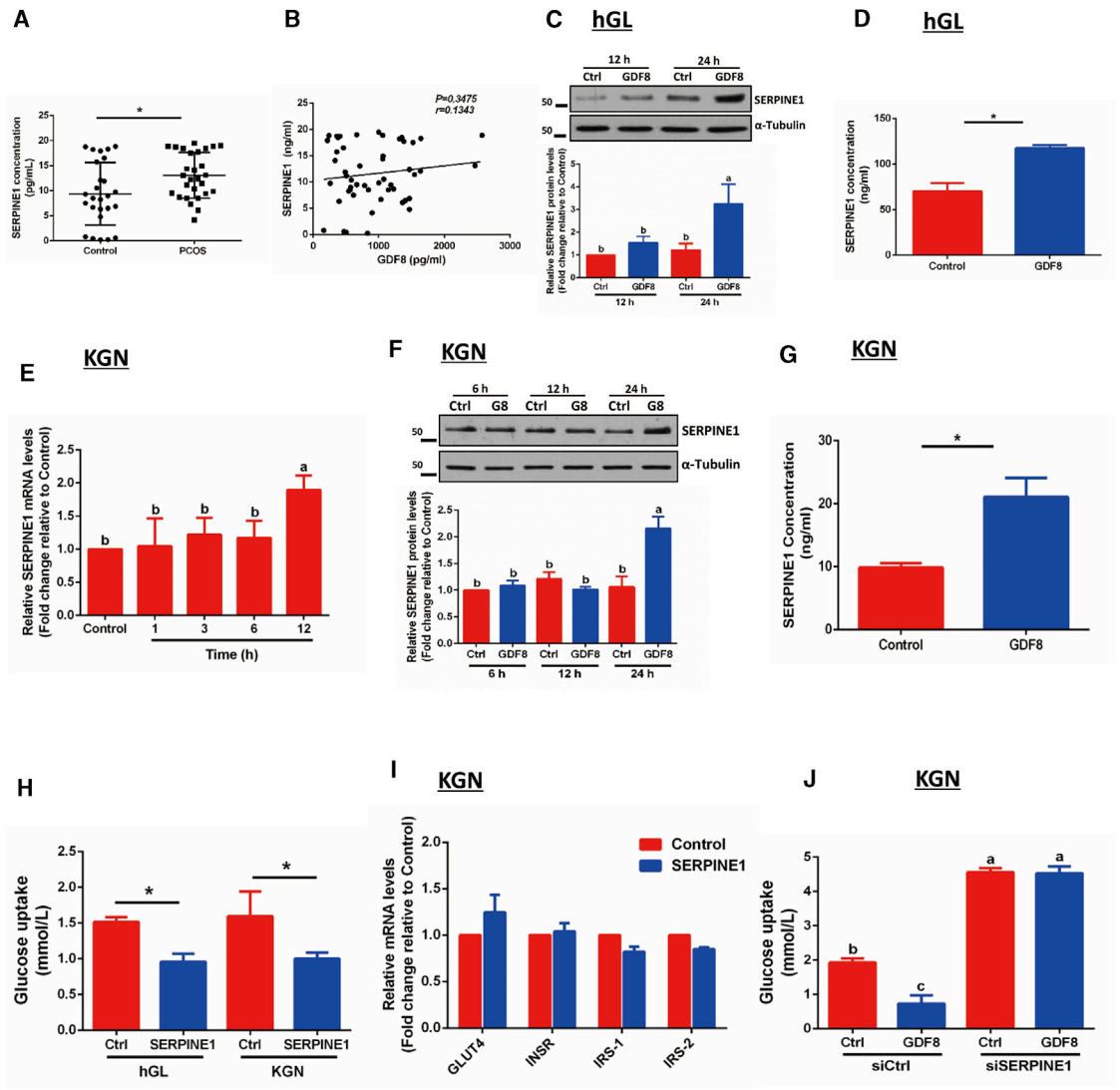

Figure 3. SERPINE1 is involved in GDF8-induced disruption of glucose metabolism in hGL cells

(A) Comparison of GDF8 levels between control and PCOS patients. (B) The correlation analysis of GDF8 concentrations with SERPINE1. (C) The hGL cells were treated with vehicle control or GDF8, and the protein level changes of SERPINE1 were detected at different time points (12 and 24 h) after GDF8 treatment. (D) The SERPINE1 concentrations were measured in hGL cells conditional culture medium after 24 h of GDF8 treatment. (E and F) The KGN cells were treated with vehicle control or GDF8, and the mRNA and protein level changes of SERPINE1 were detected by quantitative real-time RT-PCR or western blot, respectively. (G) KGN cells were treated with vehicle control or GDF8, and the accumulation level changes of SERPINE1 in conditional culture medium were measured using ELISA. (H) hGL and KGN cells were treated with vehicle control or GDF8 for 24 h and then treated with insulin (300 nM) for an additional 1 h, and the changes of glucose intake were measured. (I) hGL and KGN cells were treated with vehicle control or GDF8 for 12 h, and the gene expression changes related to the insulin signaling pathway were examined by quantitative real-time RT-PCR. (J) The KGN cells were transfected with siControl or siSERPINE1 (25 nM) for 48 h, then treated with GDF8 for an additional 24 h and subsequently treated with insulin for 1 h, and the glucose intake was detected. One-way ANOVA followed by Duncan test for multiple comparisons of means. Meanwhile, for experiments involving only two groups, the data were analyzed by the two-sample t test assuming unequal variances. $p < 0.05$ was considered statistically significant. Ctrl, control; G8, GDF8; h, hour.

blotting. Our results showed that GDF8 increased SERPINE1 protein levels at 24 h, whereas there was no effect at 12 h (Figure 3C). Meanwhile, the accumulation of SERPINE1 with GDF8 treatment in hGL cells was examined using ELISA, and the results showed that SERPINE1 production was upregulated with GDF8 treatment (Figure 3D). Moreover, immortalized human granulosa cells, named KGN cells, were utilized to further confirm the effect of GDF8 on SERPINE1 expression. Our results showed that GDF8 increased both the mRNA and protein expression levels of SERPINE1 in KGN cells (Figures 3E and 3F). The upregulation in SERPINE1 mRNA expression occurred only at 12 h, whereas GDF8 did not increase SERPINE1 mRNA expression at 1, 3, or 6 h (Figure 3E). The western blot results were similar to the qPCR

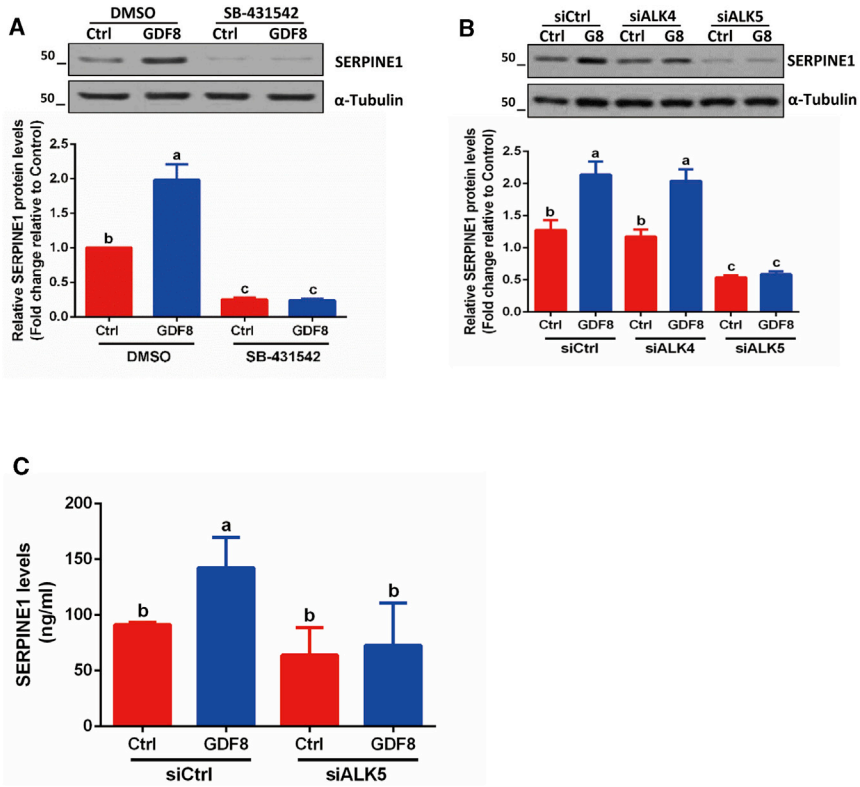

Figure 4. ALK5 mediates GDF8-induced increase of SERPINE1 in KGN cells

(A) The KGN cells were pretreated with the specific type I receptor inhibitor SB-431542 (10 μM) and then treated with GDF8 for an additional 24 h, and the protein level changes of SERPINE1 were examined by western blot. (B and C) The KGN cells were transfected with ALK4- and ALK5-specific siRNA for 48 h and then treated with GDF8 for an additional 24 h, and the changes of SERPINE1 expression and accumulation in KGN cells were detected by western blot and ELISA. One-way ANOVA followed by Duncan test for multiple comparisons of means. Meanwhile, for experiments involving only two groups, the data were analyzed by the two-sample t test assuming unequal variances. $p < 0.05$ was considered statistically significant. ALK4, activin A receptor type 1B; ALK5, transforming growth factor β receptor 1.

results, and SERPINE1 protein levels were upregulated only at 24 h, but not at the other time points (3, 6, and 12 h) after GDF8 treatment (Figure 3F). The accumulation levels of GDF8 in conditional culture medium after GDF8 treatment were also determined by ELISA, and results demonstrated that GDF8 could increase the production of SERPINE1 in KGN cells (Figure 3G). To explore the role of SERPINE1 in the regulation of granulosa cell glucose metabolism, we used the recombinant SERPINE1 proteins to treat hGL and KGN cells. Our results showed that SERPINE1 treatment significantly inhibited glucose metabolism in both hGL and KGN cells (Figure 3H). Then we further determined the effect of SERPINE1 on glucose metabolism-related gene expression. The results showed that SERPINE1 did not affect the expression of GLUT4, INR, IRS-1, and IRS-2 (Figure 3I). To further confirm that SERPINE1 is involved in GDF8-induced impairment of glucose metabolism, we utilized a small interfering RNA (siRNA)-based approach to knock down SERPINE1 expression in KGN cells. The results showed that knockdown of endogenous SERPINE1 abolished GDF8-induced impairment of glucose metabolism, indicating the negative effect of GDF8 on granulosa cell glucose metabolism (Figure 3J). The knockdown efficiency was shown in Figure S1A.

TGF-β receptor 1 is required for GDF8-induced SERPINE1 expression and secretion

In mammalian cells, GDF8-induced downstream signaling activation relies on the binding of GDF8 and its functional receptors. Generally, two TGF-β type I receptors are responsible for the activation of downstream signaling.[12] To explore the involvement of TGF-β type I receptors, we used both pharmacological and siRNA-based approaches to block the activity of these receptors. KGN cells were pretreated with SB-431542 (a potent TGF-β receptor type I receptor inhibitor) and then treated with GDF8 (30 ng/mL). Western blot results showed that SB-431542 completely blocked GDF8-induced SERPINE1 expression and secretion in KGN cells (Figure 4A). To further confirm which type I receptor participates in the effect of GDF8 on SERPINE1 expression, we knocked down endogenous type I receptors using specific siRNAs targeting activin A receptor type 1B and TGF-β receptor type I (also known as ALK4 and ALK5). As shown in Figure 4B, the GDF8-induced upregulation of SERPINE1 was completely abolished by ALK5 knockdown, whereas ALK4 knockdown did not have this effect. Moreover, the accumulation of SERPINE1 induced by GDF8 was also abolished after the knockdown of ALK5 (Figure 4C).

The SMAD2/3-SMAD4 signaling pathway mediates GDF8-induced SERPINE1 expression and secretion

After GDF8 binds to the TGF-β type I receptor, downstream SMAD2 and SMAD3 proteins are phosphorylated and form a complex, which then recruits the common mediator SMAD4. This SMAD complex rapidly translocates into cell nuclei directly or binds with other transcriptional factors to regulate target gene expression.[23] To explore the requirement of the SMAD signaling pathway in GDF8-induced SERPINE1 expression, we treated the KGN cells with GDF8 and examined the phosphorylation level changes of SMAD2 and SMAD3. The results showed that GDF8 treatment could induce the phosphorylation of both SMAD2 and SMAD3 at 30 and 60 min after GDF8 treatment (Figure 5A). Meanwhile, the involvement of ALK5 in GDF8-induced phosphorylation of SMAD2 and SMAD3 was also detected. The pretreatment of SB-431542 could completely reverse the increase of SMAD2 and SMAD3 phosphorylation levels after GDF8

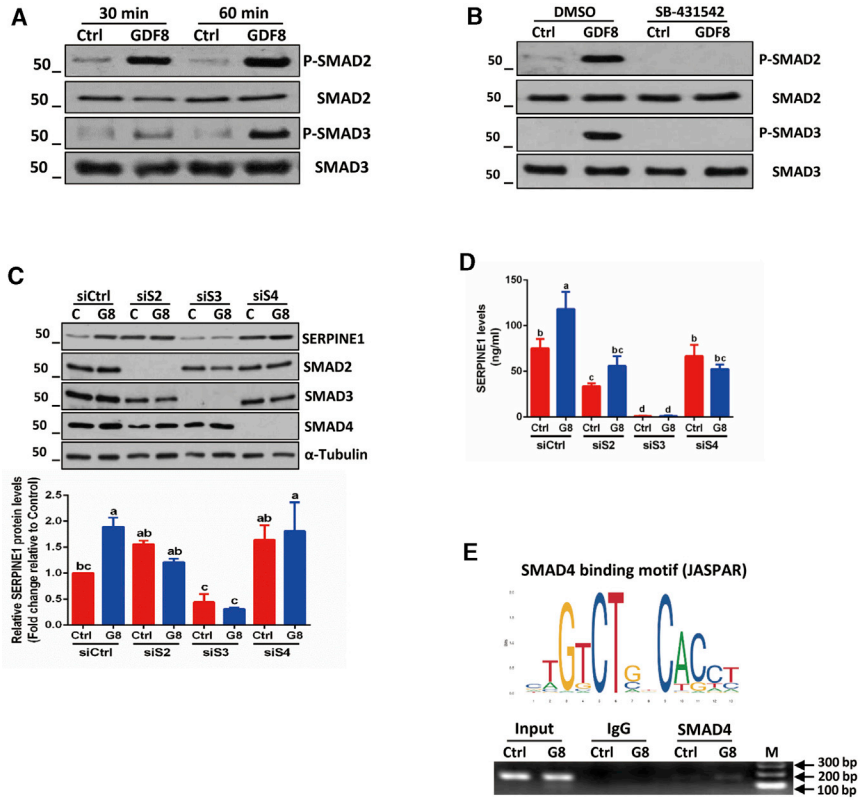

Figure 5. SMAD2/3-SMAD4 signaling pathway is required for the effect of GDF8 on SERPINE1 expression in KGN cells

(A) KGN cells were treated with GDF8, and phosphorylation level changes of SMAD2 and SMAD3 were detected at 30 and 60 min after GDF8 treatment by western blot. (B) KGN cells were treated with SB-431542 and then treated with GDF8 for an additional 30 min, and SMAD2 and SMAD3 phosphorylation level changes were examined using western blot. (C and D) KGN cells were transfected with Ctrl, SMAD2, SMAD3, and SMAD4 siRNA (25 nM), respectively. The protein and accumulation level changes of SERPINE1 were determined by western blot and ELISA, respectively. (E) The KGN cells were treated with GDF8 for 12 h. Then the binding capacity of SMAD4 on SERPINE1 promotor was examined by ChIP assay. One-way ANOVA followed by Duncan test for multiple comparisons of means. Meanwhile, for experiments involving only two groups, the data were analyzed by the two-sample t test assuming unequal variances. $p < 0.05$ was considered statistically significant. M, marker; P, phosphorylated; S2, SMAD2; S3, SMAD3; S4, SMAD4.

treatment (Figure 5B). Furthermore, the role of SMAD4 in GDF8-induced SERPINE1 expression was also determined. The specific SMAD4 siRNA was transfected into KGN cells, and the results showed that SMAD4 siRNA significantly decreased the expression of SMAD4 (Figures 5C and S1B), which reversed GDF8-induced SERPINE1 upregulation and secretion (Figure 5C). A number of studies have demonstrated that SMAD2 and SMAD3 share equal functions that mediate TGF-β superfamily member signal transduction. However, few studies consider that SMAD2 and SMAD3 have distinct and nonoverlapping functions in TGF-β1 signal transduction.[24] To determine the role of SMAD2 and SMAD3 in GDF8-induced SERPINE1 expression, we transfected KGN cells with SMAD2- or SMAD3-specific siRNA. Our results showed that both SMAD2 and SMAD3 siRNA significantly decreased SMAD2 and SMAD3 expression, respectively (Figures 5C, S1C, and S1D). Moreover, either SMAD2 or SMAD3 knockdown completely abolished GDF8-induced SERPINE1 expression, indicating that both SMAD2 and SMAD3 are required for GDF8-induced upregulation of SERPINE1 expression (Figure 5C). Furthermore, the effects of SMAD2, SMAD3, and SMAD4 knockdown on GDF8-induced SERPINE1 production in KGN cells were examined. Our results demonstrated that SMAD2, SMAD3, and SMAD4 knockdown could totally abolish the effect of GDF8 on SERPINE1 expression. Intriguingly, knockdown of SMAD3 also decreased the basal protein and accumulation levels of SERPINE1 in KGN cells (Figures 5C and 5D), indicating the necessary role of SMAD3 on basal SERPINE1 expression. Finally, the binding capacity of SMAD4 on SERPINE1 promoter was explored by chromatin immunoprecipitation (ChIP) assay. Our results demonstrated that SMAD4 could specifically bind to the SERPINE1 promoter after GDF8 treatment, indicating the transcriptional regulation effect of SMAD4 on SERPINE1 expression (Figure 5E).

The extracellular signal-regulated kinase 1/2 signaling pathway is activated by GDF8 but is not involved in GDF8-induced SERPINE1 expression

Previous studies have reported that the SMAD-independent noncanonical signaling pathway can be activated by GDF8 stimulation in multiple cell types.[22,25,26] To confirm other potential mechanisms involved in the GDF8-induced expression of SERPINE1, we detected activation of the extracellular signal-regulated kinase 1/2 (ERK1/2) signaling pathway, which has been demonstrated to mediate the effect of GDF8 on the physiology of SVOG cells.[22] Consistent with the SVOG results, we found that GDF8 increased the phosphorylation of ERK1/2 at both 30 and 60 min after GDF8 treatment in KGN cells (Figure S2A). Next, a specific ERK1/2 signaling pathway inhibitor, U0126, was used to examine the involvement of ERK1/2 in GDF8-induced SERPINE1 expression. KGN cells were pretreated with U0126 for 1 h and then treated with 30 ng/mL GDF8, and changes in SERPINE1 expression were determined by western blotting. Our results showed that inhibitor treatment did not block GDF8-induced SERPINE1 expression (Figure S2B). Moreover, the accumulation of SERPINE1 with U0126 treatment was also detected, and the results were similar to the western blot results (Figure S2C). Taken together, our results demonstrate that the ERK1/2 signaling pathway is not involved in the

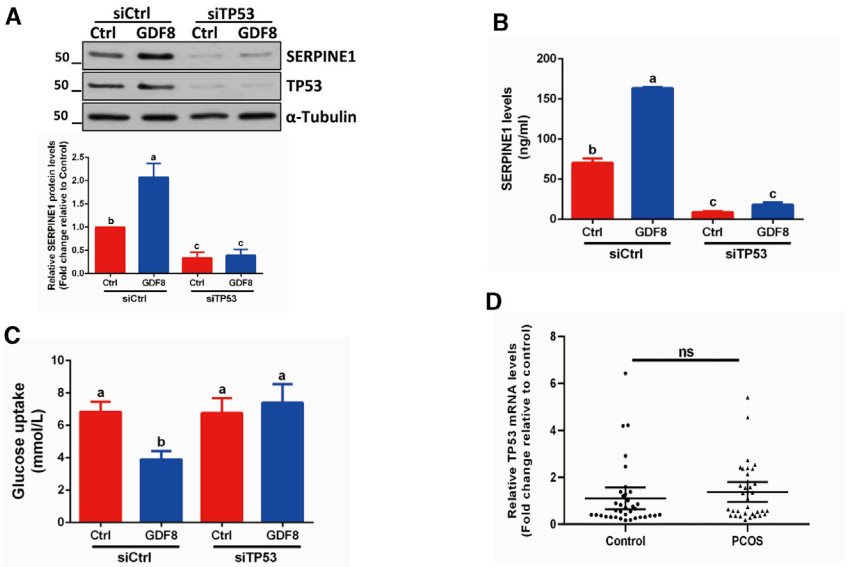

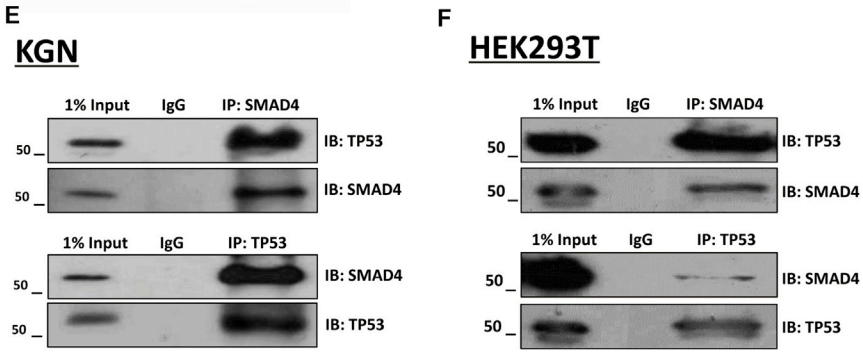

Figure 6. TP53 mediates the effect of GDF8 on SERPINE1 expression in KGN cells

(A–C) The KGN cells were transfected with the specific siRNA (25 μM) to knock down endogenous TP53 expression, and the expression (A) and accumulation (B) changes of SERPINE1 were examined by western blot and ELISA, respectively. Meanwhile, the changes of glucose intake in KGN cells were measured. (D) The mRNA expression change analysis of TP53 in granulosa cells derived from control or PCOS patients. (E and F) The KGN cells were treated with GDF8 for 24 h, and HEK293T cells were transfected with 500 ng SMAD4 and TP53 expression vectors. Then the whole-cell lysates were harvested, and the interaction of SMAD4 and TP53 was detected by co-immunoprecipitation assays. One-way ANOVA followed by Duncan test for multiple comparisons of means. Meanwhile, for experiments involving only two groups, the data were analyzed by the two-sample t test assuming unequal variances. $p < 0.05$ was considered statistically significant.

regulatory effect of GDF8 on SERPINE1 expression, even though it is activated by GDF8 in KGN cells.

TP53 is required for GDF8-induced SERPINE1 expression and secretion

Studies have shown that TP53 (also named P53) regulates SERPINE1 expression in normal and cancer cells.[27–29] In addition, TP53 binds with SMAD proteins to form a complex that regulates gene expression.[30] To confirm the expression of TP53 in human granulosa cells, we examined the mRNA and protein levels of TP53 in human and mice granulosa cells. The results showed that by using quantitative real-time RT-PCR and western blot, the cycle threshold (Ct) mean of TP53 and housekeeping gene transcriptional levels were approximately 21.35 and 17.23, respectively (Table 4). Western blot results showed TP53 protein expression levels were relatively high in hGL cells (Figure S3A). Meanwhile, similar results were also obtained in primary mice granulosa cells (Figure S3B; Table 4). Our results demonstrated that granulosa cells had relatively high TP53 expression levels. Meanwhile, it has been reported that KGN cells express the wild-type TP53.[31] To determine the involvement of TP53 in the GDF8-induced upregulation of SERPINE1 expression in granulosa cells, we transfected specific TP53 siRNA into KGN cells and examined SERPINE1 expression. Our results showed that knockdown of endogenous TP53 completely reversed the GDF8-induced upregulation of SERPINE1 expression (Figure 6A). Moreover, the secretion levels of SERPINE1 after TP53 siRNA treatment were also determined by ELISA. The results showed that the GDF8-induced accumulation of SERPINE1 was also abolished when TP53 expression was knocked down (Figure 6B). Furthermore, we also demonstrated that knockdown of endogenous TP53 completely reversed GDF8-induced glucose metabolism detected in KGN cells (Figure 6C). The knockdown efficiency of TP53 was shown in Figures 6A and S3C. Meanwhile, the additional experiments were designed to examine the expression changes of TP53 in granulosa cells between normal and PCOS patients using quantitative real-time RT-PCR. Our results showed that there was no difference of TP53 expression levels between the normal and PCOS patients (Figure 6D). These results indicate that TP53 is required for GDF8-mediated regulation of SERPINE1 expression. Meanwhile, the effects of GDF8 on TP53 expression and nuclear localization were also examined. Our results showed that GDF8 did not regulate TP53 protein expression (Figure S3D). Immunofluorescence results showed that TP53 nuclear localization did not change at 1 and 3 h after GDF8 treatment. Western blot results showed that either nucleic or cytoplasmic TP53 protein levels also were not affected after GDF8 treatment (Figures S3E and S3F). Collectively, our results demonstrated that GDF8 did not affect the nuclear localization of TP53. Furthermore, we examined TP53-SMAD complex formation using coimmunoprecipitation (coIP). Previous results showed that SMAD2/3 was rapidly phosphorylated after GDF8 treatment. It is well known that phosphorylated SMAD2/3 combines with SMAD4 to form the protein complex. Thus, SMAD4 was used as the binding protein to

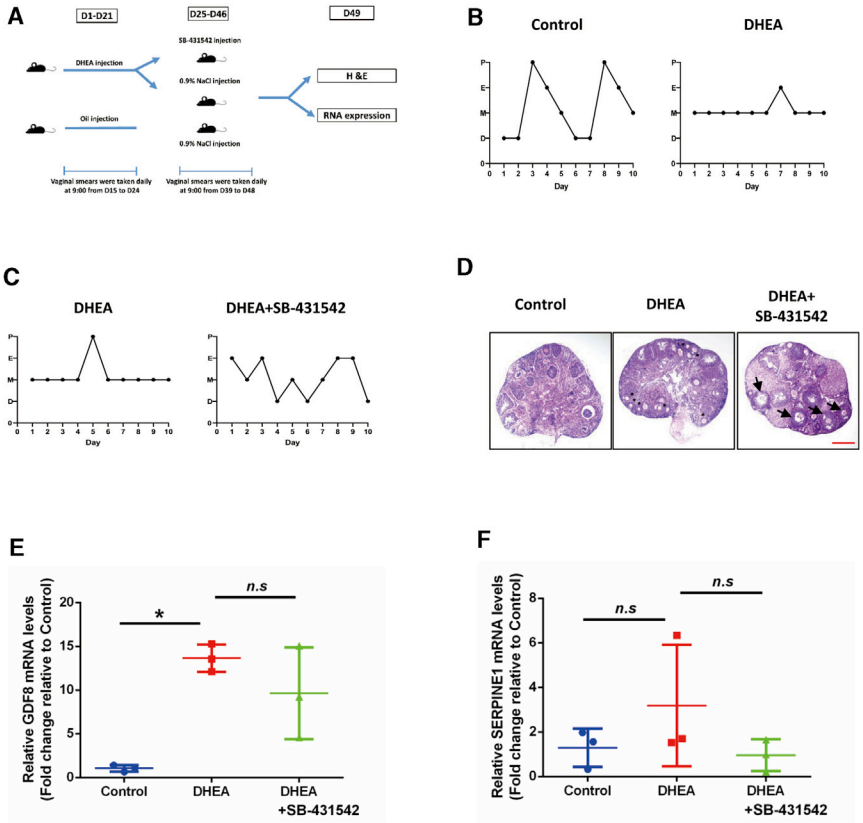

Figure 7. Effect of SB-431542 on the DHEA-induced PCOS mouse model

(A) The diagram of animal experiment procedure. (B and C) The stage analysis of mouse estrus cycle in different groups. (D) H&E staining of representative ovaries. Scale bar: 100 μm. Images are representative of three independent experiments with similar results. (E and F) The expression changes of GDF8 (E) and SERPINE1 (F) in different groups. One-way ANOVA followed by Duncan test for multiple comparisons of means. Meanwhile, for experiments involving only two groups, the data were analyzed by the two-sample t test assuming unequal variances. $p < 0.05$ was considered statistically significant. D, diestrus; E, estrus; M, metestrus; P, proestrus.

pull down TP53 in our experiment. As shown in Figure 6E, endogenous TP53 and SMAD4 coprecipitated with each other in response to GDF8 treatment in KGN cells, which demonstrated that TP53 forms a complex with SMAD2, SMAD3, and SMAD4. Meanwhile, the interaction between TP53 and SMAD4 was further validated by transient transfection of TP53 and SMAD4 plasmids in HEK293T cells (Figure 6F). Collectively, our results indicate that TP53 participates in the GDF8-induced upregulation of SERPINE1 expression and secretion by binding to the SMAD protein to form a complex.

SB-431542 alleviates DHEA-induced PCOS-like mouse phenotype

To explore the potential molecular therapeutic targets in PCOS therapy, we used the PCOS animal model. In the animal experiment, DHEA was used to induce the PCOS-like mouse model. The animal experiment procedure was shown in Figure 7A. After the continuous injection of DHEA for 14 days, the estrus cycles were determined by vaginal smear methods. Our results showed that estrus cycles were disrupted in the DHEA treatment group, whereas the mice in the control group had normal estrus cycles (Figure 7B). Based on the successful establishment of PCOS mice, we then treated PCOS mice with SB-431542 (the specific ALK5 inhibitor used in our cell study) to rescue the estrus cycle. As shown in Figure 7C, the estrus cycles in the DHEA treatment group were partially recovered. Hematoxylin and eosin (H&E) staining results showed that SB-431542 treatment significantly improved DHEA-induced PCOS-like ovaries. The polycystic ovarian morphology was alleviated, and several follicles could develop to the mature follicle (Figure 7D). Meanwhile, the expression levels of GDF8 and SERPINE1 were determined by quantitative real-time RT-PCR. The results showed that GDF8 and SERPINE1 expression levels were significantly increased in the DHEA treatment group compared with those in the control group (Figures 7E and 7F). Interestingly, although the SERPINE1 expression levels in the SB-431542 treatment group had a decreasing tendency, a p value did not reach a significant level (Figure 7F). That may be attributable to the large individual variation in the SB-431542 treatment group. Meanwhile, we also demonstrated that there was no difference in GDF8 expression between DHEA and SB-431542 treatment groups (Figure 7E). Collectively, our results highlight the validity of SB-431542 in improving the PCOS phenotype, which implied ALK5 was a potential molecular therapeutic target in PCOS therapy.

DISCUSSION

The prevalence of IR in PCOS patients is greater than 70% according to clinical investigations, suggesting the potential role of IR in PCOS development.[4] An in-depth understanding of the pathogenesis of IR in PCOS patients will be beneficial for preventing the occurrence of PCOS. In recent years, increasing evidence has suggested that glucose metabolism disorders in granulosa cells trigger the occurrence and development of PCOS. However, the underlying mechanism of defective glucose uptake in PCOS patient granulosa cells remains unknown. In the current study, we compared and analyzed the differences in GDF8 concentration in follicular fluid from PCOS and non-PCOS patients, and our results showed that the GDF8 concentrations in PCOS patient follicular fluid were comparable higher than that in non-PCOS patients. Previous studies have proved that PCOS patients have aberrantly increased serum GDF8 levels. However, these data were obtained from biochemical detection in peripheral blood, reflecting the body-wide situation.[18] Our present study indicates that the changes of

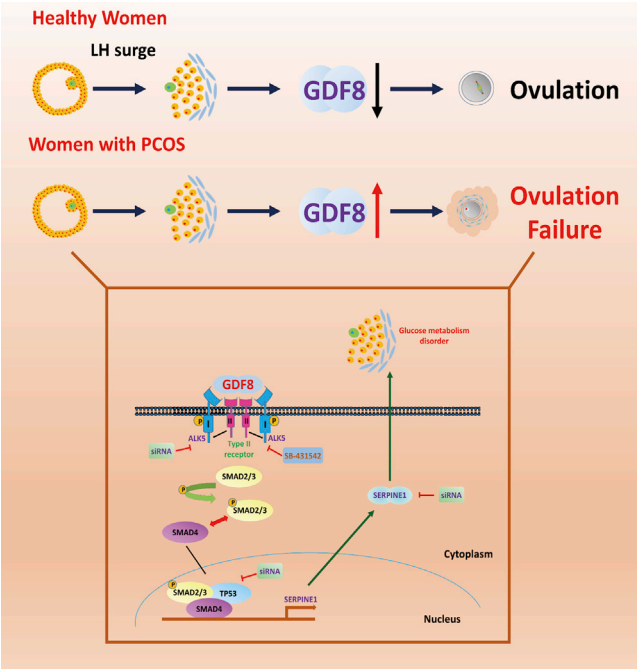

Figure 8. Schematic diagram diagram of the proposed proposed molecular molecular mechanisms mechanisms by which aberrant aberrant elevation elevation of GDF8 impairs impairs granulosagranulosa-lutein lutein cell cell glucose glucose metabolismmetabolism

Normally, the GDF8 expression is decreased after LH surge and maintained at a low level in follicular fluid to guarantee the successful ovulation. However, aberrantly increased GDF8 is present in PCOS women with IR during ovulation and impairs the granulosa cell glucose metabolism by increasing the production of SERPINE1, which leads to the defect of oocyte development and consequently causes ovulation disorder in PCOS women. GDF8 acts on hGL cells by binding to type I receptor ALK5 and activating the downstream SMAD2/3-SMAD4 signaling pathway, with an attempt to regulate SERPINE1 expression. Additionally, TP53 interacts with SMAD2/3-SMAD4 complex and mediates GDF8-induced upregulation of SERPINE1 in granulosa cells. hGL: human granulosa-lutein; ALK5: , transforming growth factor β receptor 1; hGL, human granulosa-lutein.

GDF8 in follicular fluid are similar to those in the serum of PCOS patients. Meanwhile, our results demonstrated that follicular fluid GDF8 levels were higher in obese PCOS women compared with obese non-PCOS women, and GDF8 levels were positively correlated with BMI in PCOS women. Intriguingly, we also found that PCOS women with IR had a higher level of follicular fluid GDF8 compared with that in PCOS women without IR. However, there was no difference between non-IR and IR in women without PCOS. Previous study has shown that the concentration of GDF8 in serum is not significantly different between non-obese women with or without PCOS.[18] Given the high risk for IR in obese women, previous and our current results imply that the aberrant elevation of GDF8 in PCOS women is accompanied with IR. In fact, GDF8 is a well-studied mediator of muscle development, and clinical data suggest that the levels of GDF8 are higher in obese women and positively correlated with IR, indicating the involvement of GDF8 in IR occurrence.[14,16,32,33] In our current study, we also demonstrated aberrantly increased GDF8 expression levels in granulosa cells from PCOS patients, which is consistent with our previous studies that detected significantly increased expression levels of GDF8 in PCOS ovarian granulosa cells using immunohistochemical methods.[19] Accordingly, we speculate that the high level of GDF8 in PCOS women's follicular fluid may partially attribute to the aberrant expression of GDF8 in human granulosa cells. Furthermore, we also demonstrated that the concentrations of GDF8 in follicular fluid were negatively correlated with IVF outcomes. Our findings indicate that GDF8 can be considered as a potential marker for clinical therapeutics of PCOS and evaluation of IVF outcomes.

Our previous study showed that aberrant expression of the GDF8 signaling pathway is associated with PCOS,[19] and a full understanding of the underlying molecular mechanism of GDF8-mediated gene expression will be beneficial in developing proper pharmacological therapeutic strategies for clinical applications. In the present study, our results demonstrated that GDF8 impaired insulin-dependent glucose uptake in hGL cells. However, the expression of classical insulin signaling pathway-related regulators, such as GLUT4, INSR, ISR-1, and ISR-2, was not affected by GDF8. Using RNA-seq, we identified SERPINE1 as a potential factor that may be involved in the regulatory effect of GDF8 on granulosa cell pathophysiology. SERPINE1 is a crucial mediator of extracellular matrix proteolysis and is associated with the maintenance of ovarian function and ovulation by regulating the expression of plasminogen activators (PAs).[34] Moreover, recent clinical studies have demonstrated that SERPINE1 is closely correlated with IR and is increased in serum from individuals with obesity.[6,35,36] Given the defects in glucose metabolism in PCOS, we hypothesize that SERPINE1 is involved in PCOS metabolic disorders. In the current study, we demonstrated that GDF8 significantly increased the expression of SERPINE1 in both KGN and hGL cells. Knockdown of endogenous SERPINE1 expression reversed GDF8-induced defects in glucose metabolism in KGN cells. These findings suggest that GDF8 participates in the occurrence and development of IR in PCOS patients by upregulating the expression of SERPINE1 in granulosa cells. Moreover, we acknowledge that the results of the present study were obtained from *in vitro* cell models, which have certain limitations regarding methodology. Further *in vivo* studies using animal models to verify the role of GDF8 and SERPINE1 in the occurrence and development of PCOS will be of great interest.

It is well known that the activation of the TGF-β superfamily signaling pathway is dependent on the combination of the ligand and its target receptors. Interestingly, the combination form of ligand-receptor is various in different tissues.[12] To date, seven TGF-β type I and three type II receptors have been identified.[37] ACVR2A and ACVR2B, which are type II receptors, mediate GDF8 signaling pathway activation in human granulosa cells.[38] Once binding with GDF8, TGF-β type II receptors would phosphorylate type I receptors.[12] Although there are seven type I receptors, only two type I receptors (ALK4 and ALK5) are involved in the GDF8-induced activation of downstream signaling pathways in various mammalian tissues.[12] In the most recent study, only ALK5-mediated effects of GDF8 on cell physiology and gene

Table 1. Clinical and biochemical characteristic of the woman included in this study

Characteristics	Control (n = 61)	PCOS (n = 54)
Age (y)	30	29
BMI (kg/m^2)	21.45 ± 0.32	22.29 ± 0.36
Basal FSH (mIU/mL)	6.01 ± 0.24	6.06 ± 0.21
Basal LH (mIU/mL)	5.49 ± 0.46	7.504 ± 0.84*
Basal estradiol (pg/mL)	117 ± 10.44	134.8 ± 17.48
Basal progesterone (pg/mL)	1.61 ± 0.11	1.86 ± 0.14
AFC	14.13 ± 0.47	21.2 ± 1.05
Basal testosterone (nmol/L)	0.878 ± 0.13	1.29 ± 0.10*
Basal prolactin (nmol/L)	17.97 ± 1.09	20.64 ± 2.08
Basal anti-Müllerian hormone (ng/mL)	4.09 ± 0.48	8.13 ± 0.95*
Follicular fluid GDF8 (pg/mL)	1050 ± 130.1	2220 ± 203.3*
Follicular fluid SERPINE1 (ng/mL)	9.40 ± 1.22 (n = 26)	13.08 ± 0.86* (n = 28)

Data are presented as mean ± SD values. AFC, basal antral follicle count; BMI, body mass index; FSH, follicle-stimulating hormone; LH, luteinizing hormone. *$p < 0.05$ versus control.

expression using SVOG cells (an immortalized human granulosa-lutein [hGL] cell) is reported.[39] Based on pharmacological and siRNA-mediated knockdown methods, we demonstrated that GDF8 increased SERPINE1 expression via ALK5-dependent activation of the SMAD2 and SMAD3 signaling pathways in KGN cells. Our results further confirmed that ALK5, but not ALK4, is indispensable for the function of GDF8 in human granulosa cell physiology. Surprisingly, the results from mouse C2C12 myoblasts showed that activation of the GDF8 signaling pathway relies on ALK4, but not ALK5.[40] Moreover, both ALK4 and ALK5 have been reported to be involved in GDF8-mediated cell migration in SKOV3 ovarian cancer cells.[41] These studies further confirm the multiple interactions between GDF8 and its corresponding receptors. This inconsistent receptor usage by GDF8 may be attributed to cell-type- or species-dependent differences. GDF8 preferentially uses ALK5 to regulate target gene expression in human granulosa cells. Importantly, our study also demonstrated that SB-431542, the specific inhibitor of ALK5, could significantly improve DHEA-induced PCOS-like characteristics in mice, which provided an insight of potential molecular therapeutic target in PCOS therapy.

After ligand binding, type I receptors are activated and induce the phosphorylation of downstream regulatory SMAD (R-SMAD). Generally, SMAD2 and SMAD3 are selective R-SMADs that are responsible for the effect of GDF8 on cell physiology. The siRNA-mediated knockdown results showed that either SMAD2 or SMAD3 knockdown completely reversed the GDF8-induced upregulation of SERPINE1 expression and accumulation. Our results are consistent with the conclusion obtained in the SVOG cell model that both SMAD2 and SMAD3 are required for the function of GDF8 in human granulosa cells.[22,38] SMAD4 is the common SMAD that binds with phosphorylated SMAD2 and SMAD3 to form a complex, which then translocates into the nucleus to regulate gene expression.[12] Studies in mice have shown that the conditional depletion of SMAD4 in granulosa cells causes multiple reproductive defects and decreased fertility.[42,43] In the present study, knockdown of endogenous SMAD4 completely abolished GDF8-induced upregulation of SERPINE1 expression and accumulation. These results indicate that the SMAD2/3-SMAD4 signaling pathway is indispensable for the effect of GDF8-induced upregulation of SERPINE1 expression and accumulation in human granulosa cells. In addition to the SMAD2/3 signaling pathway, several noncanonical signaling pathways are involved in the regulatory functions of TGF-β family members.[44] ERK1/2 is an ovulation mediator that is essential for luteinizing hormone (LH)-induced maturation of oocytes during the ovulation stage in mammals, and GDF8-induced activation of ERK1/2 signaling in human granulosa cells has been shown.[22,45] Similar to a previous study, our results showed that the ERK1/2 signaling pathway was also activated by GDF8. However, inhibition of the ERK1/2 signaling pathway by a specific pharmacological inhibitor did not reverse the GDF8-induced upregulation of SERPINE1 expression and accumulation in KGN cells. Taken together, our results demonstrate that the ERK1/2 signaling pathway is not involved in GDF8-induced upregulation of SERPINE1 expression and accumulation even though it can be activated by GDF8 in human granulosa cells.

Upon the nuclear translocation of the SMAD2/3-SMAD4 complex, gene transcription is regulated by direct binding with SMAD-binding elements (SBEs) on the target promoter and/or recruiting SMAD-interacting transcriptional partners.[46] Previous studies have reported that there is crosstalk between TGF-β signaling and TP53 protein.[47] In the current study, knockdown of TP53 using a specific siRNA completely abolished the GDF8-induced increase in SERPINE1 expression and accumulation in KGN cells. Our results demonstrate that TP53 is required for the regulation of SERPINE1 expression and accumulation by GDF8. In granulosa cells, TP53 is mainly working as a mediator responding to the various harmful stimulations to control the initiation of cell apoptosis.[48,49] Meanwhile, TP53 has been reported to participate in the regulation of cell proliferation and steroidogenesis in granulosa cells.[50,51] In our present study, we found the essential role of TP53 in the regulation of gene transcription, which was consistent with the previous study, which demonstrated the involvement of TP53 in regulating gene transcription in granulosa cells.[52] Importantly, clinical research reveals that TP53 polymorphisms are associated with the incidence of PCOS.[53] However, the functional role of p53 in the incidence of PCOS remains unclear, which is worth further exploration. Moreover, the detailed molecular mechanism by which TP53 participates in the regulation of the GDF8 signaling pathway was also explored in the present study. Our coIP results showed that SMAD4 interacted with TP53 after GDF8 stimulation. Our study did not demonstrate whether the interaction between SMAD4 and TP53 was direct or indirect. However, recent studies have proved that the C-terminal domain of TP53 interacts with the MH2 domain of SMAD3 when the SMAD complex transfers to the nucleus after TGF-β1 treatment in HepG2 cells.[30] Accordingly,

Table 2. Antibody information

Antibody name	Manufacturer (catalog number)	Applications (working dilution)
Anti-SERPINE1	Proteintech (13801-1-AP)	WB (1:2,000)
Anti-TP53	Proteintech (10442-1-AP)	WB (1:2,000)
Anti-α-Tubulin	Santa Cruz (sc-23948)	WB (1:5,000)
Anti-Lamin B1	Santa Cruz (sc-374015)	WB (1:500)
Anti-phospho-SMAD2$^{Ser465/467}$	Cell Signaling (3108)	WB (1:1,000)
Anti-SMAD2	Cell Signaling (3103)	WB (1:1,000)
Anti-phospho-SMAD3$^{Ser423/425}$	Cell Signaling (9520)	WB (1:1,000)
Anti-SMAD3	Cell Signaling (9523)	WB (1:1,000)
Anti-phospho-p44/42 MAPK (Erk1/2)$^{Thr202/Tyr204}$	Cell Signaling (9106)	WB (1:2,000)
Anti-p44/42 MAPK (Erk1/2)	Cell Signaling (9102)	WB (1:2,000)

MAPK, mitogen-activated protein kinase.

we hypothesize that GDF8 promotes the formation of the SMAD2/3-SMAD4-TP53 complex in human granulosa cells, most likely via the direct binding of SMAD3 and TP53. In addition, our results showed that knockdown of TP53 also dramatically decreased the basal protein expression levels of SERPINE1. Our findings indicate that TP53 may also play a key role in maintaining basal SERPINE1 levels in hGL cells. Actually, it has been well established that TP53 can recognize p53 responsive element (p53RE) sequences and bind to the proximal p53RE at the promoter of SERPINE1.[30] Further exploration is warranted to investigate whether there is the same transcriptional regulatory machinery in human granulosa cells.

In conclusion, our present study demonstrates that GDF8 concentrations in follicular fluid and expression levels in granulosa cells are significantly higher in PCOS patients than in the control group. GDF8 levels in follicular fluid are positively correlated with the number of obtained oocytes, fertilization rate, and high-quality embryo rate. GDF8 treatment impairs insulin-mediated glucose metabolism of hGL cells. RNA-seq results identified that SERPINE1 expression was upregulated with GDF8 stimulation. We also demonstrated that SERPINE1 was a mediator involved in GDF8-induced defects in glucose metabolism in hGL cells. GDF8-induced SERPINE1 expression and accumulation are mediated by ALK5-dependent activation of the SMAD2/3-SMAD4 signaling pathway. Furthermore, our results show that the ERK1/2 signaling pathway is also activated by GDF8 but is not required for the effect of GDF8 on SERPINE1 expression and accumulation in KGN cells. In addition, we also demonstrated that TP53 is involved in GDF8-induced increase in SERPINE1 expression and accumulation by binding to the SMAD2/3-SMAD4 complex (Figure 8). Finally, we demonstrated the therapeutic effect of SB-431542 in improving the DHEA-induced PCOS-like characteristics in mice. These findings provide insights into the pathophysiological role of aberrant levels of GDF8 and SERPINE1 in PCOS patient follicular fluid, which increases opportunities to use a more efficient and safe therapeutic strategy to improve intrafollicular glucose metabolism in PCOS patients.

MATERIALS AND METHODS

Ethics statement and human subjects

The study was approved by the Ethical Committee of the Women's Hospital, Zhejiang University School of Medicine, China (file no. 20180139). All participants signed a document of informed consent before participation in the study. All subjects were obtained from women (20–35 years old) undergoing IVF-embryo transfer (IVF-ET) at the center for Reproductive Medicine, Women's Hospital, Zhejiang University School of Medicine. Clinical characteristics of all the participants are shown in Table 1. All the PCOS women recruited into the PCOS group were diagnosed based on the revised Rotterdam diagnostic criteria for PCOS.[54] All patients with regular menstrual cycles and normal ovarian morphologies in the non-PCOS control group were selected because of male factor infertility and/or tubal reasons.

Establishment of DHEA-induced PCOS-like mice

All mouse studies were approved by the Zhejiang University Animal Care and Use Committee (file no. 12115). The 21-day-old female mice with C57BL/6 background were provided by the laboratory animal center of Zhejiang University and randomly divided into three groups, named control, DHEA, and DHEA+SB-431542 groups. Each group contains three to four mice. DHEA and DHEA+SB-431542 groups were first given intraperitoneal injection of DHEA for 21 days (6 mg per 100 g, dissolved in the sesame oil), whereas the control group received intraperitoneal injection of sesame oil. Then the stage of estrus cycle was determined by vaginal smear approach at 9:00 a.m. from the 14th day after the first DHEA treatment day. After 3 weeks of treatment, mice with estrus cycle disorder in the DHEA+SB-431542 group were subsequently treated with SB-431542 (100 μM) for 21 days. Meanwhile, the DHEA group was treated with saline solution. After 2 weeks of treatment, the stages of estrus cycle were determined by vaginal smear approach at 9:00 a.m. until 10 days. Then all the mice were sacrificed, and ovary tissues were collected. One side of ovary was fixed in 4% paraformaldehyde until H&E staining. The other side of ovary was lysed in TRIzol buffer to extract mRNA.

Antibodies and reagents

All the antibodies used in the study were listed in Table 2. Recombinant human GDF8 (788-G8), GDF8 Quantikine ELISA Kit (DGDF80), and Human SERPIN1 Quantikine ELISA Kit (DSE100) were purchased from R&D Systems (MN, USA). Horseradish peroxidase (HRP)-conjugated goat anti-rabbit (1706515) and goat anti-mouse (1706516) secondary antibodies and Clarity Max Western ECL Substrate (1705062) were obtained from Bio-Rad (CA, USA). SB-431542 (S1067) and U0126 (S1102) inhibitors were obtained from Selleck (Shanghai, China).

Table 3. Primer used in this study

Gene	Primer	Sequence (5′–3′)
GDF8	Forward	TTTTACCCAAAGCTCCTCCA
	reverse	GAGTCTCGACGGGTCTCAAA
SERPINE1	forward	TGGTTCTGCCCAAGTTCTCC
	reverse	GACTGTTCCTGTGGGGTTGT
GLUT4	forward	CTCTCTGGCATCAATGCTGT
	reverse	ACCGAGACCAAGGTGAAGAC
INSR	forward	TGCTGTATGAAGTGAGTTATCGG
	reverse	TGTCACGTAGAAATAGGTGGGTT
IRS-1	forward	GATTTAAGCGCCTATGCCA
	reverse	GAAGATATGAGGTCCTAGTTGTGAA
IRS-2	forward	GCATTGACTTCTTGTCCCACC
	reverse	CGGGCTGAAACAGTGCTGA
EXT1	forward	TAAGGAGCGGTGGGGATACA
	reverse	AGTGGATCAGCGGCATGTAG
HMGCR	forward	TGCAGCAAACATTGTCACCG
	reverse	CCATTACGGTCCCACACACA
BUB1	forward	GAAGCCCACATGCAGAGCTA
	reverse	CCAGGCAATGTACAGAGGGG
VCAN	forward	GAACCAGACAGGCTTCCCTC
	reverse	TGATGCAGTTTCTGCGAGGA
SH3RF2	forward	CAGCACACCTTCTGCAAACC
	reverse	GTTGGAAAACACAGGCGTCC
BOLA2B	forward	CATGTGGAGGTGGAGGACAC
	reverse	CAGCCTGTGTCTCTGAAGCA
GAPDH	forward	ATGGAAATCCCATCACCATCTT
	reverse	CGCCCCACTTGATTTTGG

Cell culture and follicular fluid preparation

All patients underwent a controlled ovarian stimulation protocol, and the mixture of follicular contents was obtained from the matching size dominant follicles (18–20 mm). After oocytes were retrieved, follicular fluid mixture was collected and primary hGL cells were purified by using density centrifugation from follicular aspirates as previously described.[55,56] Purified hGL cells were seeded to 12-well plates according to 2×10^5 cells per well density in DMEM/F12 (Sigma, Shanghai, China) culture medium supplied with 5% fetal bovine serum (BI, Cromwell, CT, USA), 100 U/mL penicillin (Life Technologies, Shanghai, China), 100 mg/mL streptomycin sulfate (Life Technologies), and 1× GlutaMAX (Life Technologies). Meanwhile, the follicular fluid was centrifuged and collected after the cumulus oocyte complex was retrieved and stored at −80°C until measurement. In the present study, a granulosa cell tumor-derived cell line (KGN) was utilized to explore the function of GDF8 on granulosa cell glucose metabolism and the underlying mechanism. KGN cells were seeded to six-well plates according to 2×10^5 cells/well density in DMEM/F12 culture medium supplied with 5% fetal bovine serum. All the cell models used in this study were cultured in a humidified atmosphere of 5% CO_2 and 95% air at 37°C, and the cell culture medium was changed every 2 days in all experiments.

Transcriptome analysis

Total mRNA was extracted from control or GDF8-treated hGL cells according to the manufacturer's instructions (Thermo Fisher Scientific). The mRNA was then converted into double-strand cDNA using SuperScript III Reverse Transcriptase (Takara, Japan). Three replicates were rendered for RNA-seq library preparation, with the utilization of NEB Next Ultra Directional RNA Library Prep Kit for Illumina (NEB, USA) according to the manufacturer's protocol. Illumina HiSeq 2500 system was used to perform the ensuing RNA-seq library sequencing. The expression level of a certain gene was quantified as fragments per kilobase of transcript per million mapped reads (FPKMs). The differential gene expression was identified using DESeq2 software. In our study, Benjamini and Hochberg's approach for controlling the false discovery rate (FDR) was utilized to adjust the p value of detected transcripts. Significant differentially expressed genes (DEGs) were examined with padj (adjusted p value) <0.05. Meanwhile, absolute fold change of 2 was set as the threshold for significantly differential expression. DEGs were further analyzed using GO enrichment analysis by the cluster Profiler R package, in which gene length bias was corrected. The DO database was utilized to describe human genes function and diseases. p values <0.05 were considered significantly enriched by differentially expressed genes in GO enrichment and DO database analysis.

Quantitative real-time RT-PCR

Total RNAs were exacted with TRIzol reagents (Takara, Japan) according to the instructions. A total of 3 μg RNA was reverse transcribed into the complementary DNA (cDNA) using PrimeScript RT reagent Kit (Takara). Each 20 μL sample volume containing 10 μL of 2× SYBR Green PCR Master Mix (Takara), 250 nM each specific primer, and 20 ng of cDNA was determined by qPCR. The specific primers used in qPCR were shown in Table 3. The triplicate measurements of each cDNA sample were set, and qPCR results were calculated by obtaining the mean value of triplicate results. The relative expression levels of target gene mRNA were displayed using the comparative Ct method with the $2^{-\Delta Delta;Ct}$ values formula, and GAPDH was used as a reference gene (Table 4). All primers used in this study passed the validation test.

Western blot analysis

After the treatment, all the cells were lysed in cell lysis buffer (Cell Signaling Technology), and the protein concentration of the sample was determined using Pierce Rapid Gold BCA kit according to the manufacturer's instructions (Thermo Fisher, USA). Equal amounts of protein were loaded and separated using sodium dodecyl sulfate-polyacrylamide gel electrophoresis (SDS-PAGE) analysis. After that, the proteins were transferred onto polyvinylidene difluoride (PVDF) membranes (Bio-Rad, USA), and then the membranes were blocked by Tris-buffered saline (TBS) containing 5% non-fat dry milk for 1 h at room temperature and incubated overnight at 4°C with corresponding primary antibodies. The next day, the

Table 4. Ct value of TP53 in quantitative real-time RT-PCR analysis

Species	Sample	Gene	Ct value
Human	1	TP53	21.38
		GAPDH	15.63
	2	TP53	21.38
		GAPDH	20.68
	3	TP53	21.29
		GAPDH	15.37
Mouse	1	Trp53	21.04
		Actin	17.59
	2	Trp53	20.91
		Actin	16.70
	3	Trp53	20.84
		Actin	17.15

membranes were washed with TBS for 1 h and then incubated in the appropriate HRP-conjugated secondary antibody for 30 min. Similarly, the membranes were washed with TBS for 1 h after secondary antibody incubation. Finally, the immunoreactive bands were detected with an enhanced chemiluminescent substrate (Bio-Rad) and X-ray film. The intensities of the bands were quantified with Image-Pro Plus software (v.4.5; Media Cybernetics, USA).

siRNA transfection

Cells were cultured at approximately 70% density and transfected with 25 nM corresponding siRNA products generally consisting of pools of three to five target-specific 19–25 nt siRNAs or siCONTROL nontargeting pool siRNA as the transfection control (Santa Cruz, USA) using Lipofectamine RNA iMAX according to the manufacturer's instructions (Life Technologies). The knockdown efficiency of the target siRNA was detected by quantitative real-time RT-PCR or western blot analysis.

Co-immunoprecipitation experiments

KGN cells were treated with GDF8, and HEK293T cells were transfected with SMAD4 and TP53 expression vectors. Co-immunoprecipitation (coIP) assay for SMAD4 and TP53 was performed by lysing KGN and HEK293T cells with NETN300 lysis buffer. Cell lysates were mixed with protein A beads (Santa Cruz) and SMAD4 or TP53 antibody, respectively, and incubated in the shaker for 2 h at 4°C temperature. A rabbit IgG antibody was utilized as negative control. Then the beads were washed three times using NETN100 buffer, and the final immunoprecipitates were degenerated in loading buffer and further stored at −80°C until use by the western blot analysis experiment.

ChIP

The binding capacity of SMAD4 on SERPINE1 promoter was examined by ChIP assay using SimpleChIP Plus Enzymatic Chromatin IP Kit according to the manufacturer's instructions (9004; CST). The specific primer used for SMAD4 binding site within SERPINE1 promotor was forward: 5′-CAGGGATGAGGGAAAGAC-3′; reverse: 5′-GACCACCTCCAGGAAAGA-3′. The purified DNA was subjected to PCR amplification. The PCR products were resolved by electrophoresis on a 1% agarose gel and stained by ethidium bromide.

Immunofluorescence

KGN cells were fixed with 4% paraformaldehyde at room temperature for 10 min after the treatment. Then the cells were permeabilized with 0.5% Triton X-100 in PBS for 20 min, and subsequently 5% BSA blocked the cells for 30 min. Cells were incubated with the first antibody for 1 h at room temperature and then washed three times with PBS. Then cells were incubated with the second antibody for an additional 30 min and washed three times using PBS. Finally, the cells were incubated into Hoechst 33342 for 5 min. Imaging was performed on the Olympus IX73 microscope.

ELISA measurement

The conditional cell cultured medium with treatment or follicular fluid samples were collected and stored at −80°C if not detected immediately. The concentrations of GDF8 and SERPINE1 in cell culture medium or follicular fluid were determined by ELISA analysis according to the manufacturer's instructions (R&D Systems). The GDF8 and SERPINE1 levels in conditional cultured medium were normalized to the protein concentration of each cell lysate. The normalized GDF8 and SERPINE1 levels for each treated sample are displayed as percentages of the normalized control levels.

Statistical analysis

The data were displayed as the mean ± SEM of at least three independent experiments. PRISM 6.0 software (GraphPad Software Inc, USA) was used to perform a one-way analysis of variance (ANOVA) followed by Duncan test for multiple comparisons of means. Meanwhile, for experiments involving only two groups, the data were analyzed by SPSS 11.0 software (IBM, USA) with a two-sample t test assuming unequal variances. $p < 0.05$ was considered statistically significant.

SUPPLEMENTAL INFORMATION

Supplemental Information can be found online at https://doi.org/10.1016/j.omtn.2020.11.005.

ACKNOWLEDGMENTS

This research was supported by the National Key Research and Development Program of China (grant 2018YFC1003201), Natural Science Foundation of China (grant 81873819), Program for Key Subjects of Zhejiang Province in Medicine and Hygiene (to Y.M.Z.), and National Natural Science Foundation of China (grant 81901443 to L.B.).

AUTHOR CONTRIBUTIONS

L.B. and Y.Z. conceived the project and designed the experiments. L.B. and W.W. performed and analyzed the bulk of the experiments. Y.X. performed and analyzed the RNA-seq and ELISA. S. Wang performed collection of clinical samples and patient information. S. Wan

helped to perform the experiments. W.W. wrote the manuscript, and L.B. and Y.Z. revised it.

DECLARATION OF INTERESTS

The authors declare no competing interests.

REFERENCES

1. Franks, S. (1995). Polycystic ovary syndrome. N. Engl J. Med. *333*, 853–861.
2. Diamanti-Kandarakis, E., and Dunaif, A. (2012). Insulin resistance and the polycystic ovary syndrome revisited: an update on mechanisms and implications. Endocr. Rev. *33*, 981–1030.
3. Yildiz, B.O., Knochenhauer, E.S., and Azziz, R. (2008). Impact of obesity on the risk for polycystic ovary syndrome. J. Clin. Endocrinol. Metab. *93*, 162–168.
4. DeUgarte, C.M., Bartolucci, A.A., and Azziz, R. (2005). Prevalence of insulin resistance in the polycystic ovary syndrome using the homeostasis model assessment. Fertil. Steril. *83*, 1454–1460.
5. Kahn, C.R. (1985). The molecular mechanism of insulin action. Annu. Rev. Med. *36*, 429–451.
6. Martínez-García, M.A., Moncayo, S., Insenser, M., Álvarez-Blasco, F., Luque-Ramírez, M., and Escobar-Morreale, H.F. (2019). Metabolic Cytokines at Fasting and During Macronutrient Challenges: Influence of Obesity, Female Androgen Excess and Sex. Nutrients *11*, 2566.
7. Zhao, S., Xu, H., Cui, Y., Wang, W., Qin, Y., You, L., Chan, W.Y., Sun, Y., and Chen, Z.J. (2016). Metabolic actions of insulin in ovarian granulosa cells were unaffected by hyperandrogenism. Endocrine *53*, 823–830.
8. Rice, S., Christoforidis, N., Gadd, C., Nikolaou, D., Seyani, L., Donaldson, A., Margara, R., Hardy, K., and Franks, S. (2005). Impaired insulin-dependent glucose metabolism in granulosa-lutein cells from anovulatory women with polycystic ovaries. Hum. Reprod. *20*, 373–381.
9. Gougeon, A. (1996). Regulation of ovarian follicular development in primates: facts and hypotheses. Endocr. Rev. *17*, 121–155.
10. Purcell, S.H., Chi, M.M., Lanzendorf, S., and Moley, K.H. (2012). Insulin-stimulated glucose uptake occurs in specialized cells within the cumulus oocyte complex. Endocrinology *153*, 2444–2454.
11. McPherron, A.C., Lawler, A.M., and Lee, S.J. (1997). Regulation of skeletal muscle mass in mice by a new TGF-beta superfamily member. Nature *387*, 83–90.
12. Chang, H.M., Qiao, J., and Leung, P.C. (2016). Oocyte-somatic cell interactions in the human ovary-novel role of bone morphogenetic proteins and growth differentiation factors. Hum. Reprod. Update *23*, 1–18.
13. McPherron, A.C., and Lee, S.J. (2002). Suppression of body fat accumulation in myostatin-deficient mice. J. Clin. Invest. *109*, 595–601.
14. Park, J.J., Berggren, J.R., Hulver, M.W., Houmard, J.A., and Hoffman, E.P. (2006). GRB14, GPD1, and GDF8 as potential network collaborators in weight loss-induced improvements in insulin action in human skeletal muscle. Physiol. Genomics *27*, 114–121.
15. Zamani, N., and Brown, C.W. (2011). Emerging roles for the transforming growth factor-beta superfamily in regulating adiposity and energy expenditure. Endocr. Rev. *32*, 387–403.
16. Zhang, C., McFarlane, C., Lokireddy, S., Bonala, S., Ge, X., Masuda, S., Gluckman, P.D., Sharma, M., and Kambadur, R. (2011). Myostatin-deficient mice exhibit reduced insulin resistance through activating the AMP-activated protein kinase signalling pathway. Diabetologia *54*, 1491–1501.
17. Guo, J., Tian, T., Lu, D., Xia, G., Wang, H., and Dong, M. (2012). Alterations of maternal serum and placental follistatin-like 3 and myostatin in pre-eclampsia. J. Obstet. Gynaecol. Res. *38*, 988–996.
18. Chen, M.J., Han, D.S., Yang, J.H., Yang, Y.S., Ho, H.N., and Yang, W.S. (2012). Myostatin and its association with abdominal obesity, androgen and follistatin levels in women with polycystic ovary syndrome. Hum. Reprod. *27*, 2476–2483.
19. Lin, T.T., Chang, H.M., Hu, X.L., Leung, P.C.K., and Zhu, Y.M. (2018). Follicular localization of growth differentiation factor 8 and its receptors in normal and polycystic ovary syndrome ovaries. Biol. Reprod. *98*, 683–694.
20. Qiao, J., and Feng, H.L. (2011). Extra- and intra-ovarian factors in polycystic ovary syndrome: impact on oocyte maturation and embryo developmental competence. Hum. Reprod. Update *17*, 17–33.
21. Guo, T., Jou, W., Chanturiya, T., Portas, J., Gavrilova, O., and McPherron, A.C. (2009). Myostatin inhibition in muscle, but not adipose tissue, decreases fat mass and improves insulin sensitivity. PLoS ONE *4*, e4937.
22. Fang, L., Chang, H.M., Cheng, J.C., Yu, Y., Leung, P.C., and Sun, Y.P. (2015). Growth Differentiation Factor-8 Decreases StAR Expression Through ALK5-Mediated Smad3 and ERK1/2 Signaling Pathways in Luteinized Human Granulosa Cells. Endocrinology *156*, 4684–4694.
23. Heldin, C.H., Miyazono, K., and ten Dijke, P. (1997). TGF-beta signalling from cell membrane to nucleus through SMAD proteins. Nature *390*, 465–471.
24. Brown, K.A., Pietenpol, J.A., and Moses, H.L. (2007). A tale of two proteins: differential roles and regulation of Smad2 and Smad3 in TGF-beta signaling. J. Cell. Biochem. *101*, 9–33.
25. Li, F., Yang, H., Duan, Y., and Yin, Y. (2011). Myostatin regulates preadipocyte differentiation and lipid metabolism of adipocyte via ERK1/2. Cell Biol. Int. *35*, 1141–1146.
26. McFarlane, C., Hennebry, A., Thomas, M., Plummer, E., Ling, N., Sharma, M., and Kambadur, R. (2008). Myostatin signals through Pax7 to regulate satellite cell self-renewal. Exp. Cell Res. *314*, 317–329.
27. Szołtysek, K., Janus, P., Zając, G., Stokowy, T., Walaszczyk, A., Widłak, W., Wojtaś, B., Gielniewski, B., Cockell, S., Perkins, N.D., et al. (2018). RRAD, IL4I1, CDKN1A, and SERPINE1 genes are potentially co-regulated by NF-κB and p53 transcription factors in cells exposed to high doses of ionizing radiation. BMC Genomics *19*, 813.
28. Horikawa, I., Park, K.Y., Isogaya, K., Hiyoshi, Y., Li, H., Anami, K., Robles, A.I., Mondal, A.M., Fujita, K., Serrano, M., and Harris, C.C. (2017). Δ133p53 represses p53-inducible senescence genes and enhances the generation of human induced pluripotent stem cells. Cell Death Differ. *24*, 1017–1028.
29. Lim, S., Hung, A.C., and Porter, A.G. (2009). Focused PCR screen reveals p53 dependence of nitric oxide-induced apoptosis and up-regulation of maspin and plasminogen activator inhibitor-1 in tumor cells. Mol. Cancer Res. *7*, 55–66.
30. Kawarada, Y., Inoue, Y., Kawasaki, F., Fukuura, K., Sato, K., Tanaka, T., Itoh, Y., and Hayashi, H. (2016). TGF-β induces p53/Smads complex formation in the PAI-1 promoter to activate transcription. Sci. Rep. *6*, 35483.
31. Woods, D.C., Alvarez, C., and Johnson, A.L. (2008). Cisplatin-mediated sensitivity to TRAIL-induced cell death in human granulosa tumor cells. Gynecol. Oncol. *108*, 632–640.
32. Amor, M., Itariu, B.K., Moreno-Viedma, V., Keindl, M., Jürets, A., Prager, G., Langer, F., Grablowitz, V., Zeyda, M., and Stulnig, T.M. (2019). Serum Myostatin is Upregulated in Obesity and Correlates with Insulin Resistance in Humans. Exp. Clin. Endocrinol. Diabetes *127*, 550–556.
33. Reisz-Porszasz, S., Bhasin, S., Artaza, J.N., Shen, R., Sinha-Hikim, I., Hogue, A., Fielder, T.J., and Gonzalez-Cadavid, N.F. (2003). Lower skeletal muscle mass in male transgenic mice with muscle-specific overexpression of myostatin. Am. J. Physiol. Endocrinol. Metab. *285*, E876–E888.
34. Liu, Y.X. (2004). Plasminogen activator/plasminogen activator inhibitors in ovarian physiology. Front. Biosci. *9*, 3356–3373.
35. Carratala, A., Martinez-Hervas, S., Rodriguez-Borja, E., Benito, E., Real, J.T., Saez, G.T., Carmena, R., and Ascaso, J.F. (2018). PAI-1 levels are related to insulin resistance and carotid atherosclerosis in subjects with familial combined hyperlipidemia. J. Investig. Med. *66*, 17–21.
36. Schrover, I.M., van der Graaf, Y., Spiering, W., and Visseren, F.L.; SMART study group (2018). The relation between body fat distribution, plasma concentrations of adipokines and the metabolic syndrome in patients with clinically manifest vascular disease. Eur. J. Prev. Cardiol. *25*, 1548–1557.
37. Salazar, V.S., Gamer, L.W., and Rosen, V. (2016). BMP signalling in skeletal development, disease and repair. Nat. Rev. Endocrinol. *12*, 203–221.

38. Chang, H.M., Fang, L., Cheng, J.C., Klausen, C., Sun, Y.P., and Leung, P.C. (2015). Growth differentiation factor 8 down-regulates pentraxin 3 in human granulosa cells. Mol. Cell. Endocrinol. *404*, 82–90.

39. Chang, H.M., Fang, Y., Liu, P.P., Cheng, J.C., Yang, X., and Leung, P.C. (2016). Connective tissue growth factor mediates growth differentiation factor 8-induced increase of lysyl oxidase activity in human granulosa-lutein cells. Mol. Cell. Endocrinol. *434*, 186–198.

40. Kemaladewi, D.U., de Gorter, D.J., Aartsma-Rus, A., van Ommen, G.J., ten Dijke, P., 't Hoen, P.A., and Hoogaars, W.M. (2012). Cell-type specific regulation of myostatin signaling. FASEB J. *26*, 1462–1472.

41. Zhao, J., Klausen, C., Xiong, S., Cheng, J.C., Chang, H.M., and Leung, P.C. (2016). Growth differentiation factor 8 induces SKOV3 ovarian cancer cell migration and E-cadherin down-regulation. Cell. Signal. *28*, 1615–1622.

42. Pangas, S.A., Li, X., Robertson, E.J., and Matzuk, M.M. (2006). Premature luteinization and cumulus cell defects in ovarian-specific Smad4 knockout mice. Mol. Endocrinol. *20*, 1406–1422.

43. Yu, C., Zhang, Y.L., and Fan, H.Y. (2013). Selective Smad4 knockout in ovarian preovulatory follicles results in multiple defects in ovulation. Mol. Endocrinol. *27*, 966–978.

44. Heldin, C.H., and Moustakas, A. (2016). Signaling Receptors for TGF-β Family Members. Cold Spring Harb. Perspect. Biol. *8*, a022053.

45. Fan, H.Y., Liu, Z., Shimada, M., Sterneck, E., Johnson, P.F., Hedrick, S.M., and Richards, J.S. (2009). MAPK3/1 (ERK1/2) in ovarian granulosa cells are essential for female fertility. Science *324*, 938–941.

46. Hill, C.S. (2016). Transcriptional Control by the SMADs. Cold Spring Harb. Perspect. Biol. *8*, a022079.

47. Dupont, S., Zacchigna, L., Adorno, M., Soligo, S., Volpin, D., Piccolo, S., and Cordenonsi, M. (2004). Convergence of p53 and TGF-beta signaling networks. Cancer Lett. *213*, 129–138.

48. Amsterdam, A., Sasson, R., Keren-Tal, I., Aharoni, D., Dantes, A., Rimon, E., Land, A., Cohen, T., Dor, Y., and Hirsh, L. (2003). Alternative pathways of ovarian apoptosis: death for life. Biochem. Pharmacol. *66*, 1355–1362.

49. Amsterdam, A., Keren-Tal, I., and Aharoni, D. (1996). Cross-talk between cAMP and p53-generated signals in induction of differentiation and apoptosis in steroidogenic granulosa cells. Steroids *61*, 252–256.

50. Tao, H., Xiong, Q., Ji, Z., Zhang, F., Liu, Y., and Chen, M. (2019). NFAT5 is Regulated by p53/miR-27a Signal Axis and Promotes Mouse Ovarian Granulosa Cells Proliferation. Int. J. Biol. Sci. *15*, 287–297.

51. Liang, M., Yao, G., Yin, M., Lü, M., Tian, H., Liu, L., Lian, J., Huang, X., and Sun, F. (2013). Transcriptional cooperation between p53 and NF-κB p65 regulates microRNA-224 transcription in mouse ovarian granulosa cells. Mol. Cell. Endocrinol. *370*, 119–129.

52. Haraguchi, H., Hirota, Y., Saito-Fujita, T., Tanaka, T., Shimizu-Hirota, R., Harada, M., Akaeda, S., Hiraoka, T., Matsuo, M., Matsumoto, L., et al. (2019). Mdm2-p53-SF1 pathway in ovarian granulosa cells directs ovulation and fertilization by conditioning oocyte quality. FASEB J. *33*, 2610–2620.

53. Siddamalla, S., Reddy, T.V., Govatati, S., Guruvaiah, P., Deenadayal, M., Shivaji, S., and Bhanoori, M. (2018). Influence of tumour suppressor gene (TP53, BRCA1 and BRCA2) polymorphisms on polycystic ovary syndrome in South Indian women. Eur. J. Obstet. Gynecol. Reprod. Biol. *227*, 13–18.

54. Rotterdam ESHRE/ASRM-Sponsored PCOS consensus workshop group (2004). Revised 2003 consensus on diagnostic criteria and long-term health risks related to polycystic ovary syndrome (PCOS). Hum. Reprod. *19*, 41–47.

55. Bai, L., Chang, H.M., Cheng, J.C., Chu, G., Leung, P.C.K., and Yang, G. (2017). ALK2/ALK3-BMPR2/ACVR2A Mediate BMP2-Induced Downregulation of Pentraxin 3 Expression in Human Granulosa-Lutein Cells. Endocrinology *158*, 3501–3511.

56. Chang, H.M., Fang, L., Cheng, J.C., Taylor, E.L., Sun, Y.P., and Leung, P.C. (2016). Effects of growth differentiation factor 8 on steroidogenesis in human granulosa-lutein cells. Fertil. Steril. *105*, 520–528.